PCCP

Accepted Manuscript

ROYAL SOCIETY OF CHEMISTRY

www.rsc.org/pccp

PCCP

RSCPublishing

ARTICLE

Adsorptive desulfurization with CPO-27/MOF-74: an experimental and computational investigation

Cite this: DOI: 10.1039/x0xx00000x

Received 00th februari 2015,
Accepted 00thfebruari 2015

DOI: 10.1039/x0xx00000x

www.rsc.org/

Ben Van de Voorde,[a] Markéta Hezinová,[b] Jeroen Lannoeye,[a] Annelies Vandekerkhove,[a] Bartosz Marszalek,[c] Barbara Gil,[c] Isabelle Beurroies,[d] Petr Nachtigall[b] and Dirk De Vos[a]*

By combining experimental adsorption isotherms, microcalorimetric data, infrared spectroscopy and quantum chemical calculations the adsorption behaviour of the CPO-27/MOF-74 series (Ni, Co, Mg, Cu, Zn) in the desulfurization of fuels is evaluated. The results show a clear influence of the metal ion on the adsorption capacity and affinity for S-heterocyclic compounds, with CPO-27(Ni) being the best performing material both in capacity and affinity. The microcalorimetric data and infrared spectroscopy confirm the high affinity of CPO-27(Ni) for thiophene and similar compounds, while the computational data reveal that the origin for this outstanding adsorption performance is the strong sulfur-metal interaction.

Introduction

Metal-Organic Frameworks (MOFs) are a class of materials combining both organic and inorganic building blocks into a uniform framework.[1] This leads to materials with large porosities, high specific surface areas, well defined pore geometries and accessible open metal sites; all these properties are important for adsorptive applications.[2,3] In the field of adsorptive separations in both liquid and gas phase, MOFs have shown to be excellent materials.[4–6] Hence they have been studied as designer adsorbents in the adsorptive desulfurization of fuels.[7–9] Due to the more stringent regulations on S concentrations (< 10 ppm S), desulfurization of fuels remains an important field, especially because of the increasing sourness of fossil resources.[10] Not only does the combustion of sulfur compounds lead to the emission of sulfur oxide gases and the formation of acid rain, automobiles are also adversely affected by presence of sulfur, as these compounds may have a deleterious effect on the efficiency of exhaust catalysts, such as Cu^{2+} or Fe^{3+} based DeNOx catalysts.[11]

Presently, the removal of sulfur from fuels is accomplished with the hydrodesulfurization (HDS) technology. Using a solid CoMo catalyst the sulfur compounds are hydrogenated to H2S at high temperature and pressure.[12] Not only is this process a very costly one; the efficient removal of bulky sulfur molecules like dibenzothiophene (DBT) and 4,6-dimethyldibenzothiophene (DMDBT) is not possible.[11,13] An attractive alternative would be the deep adsorptive desulfurisation with porous solids, like metal-organic frameworks.[8] In one of the first studies published on adsorptive desulfurisation with MOFs, Matzger and co-workers evaluated different Cu-MOFs for the adsorption of several S-heteroaromatics. MOF-505 was able to adsorb up to 3.9 wt % sulfur of DBT out of a iso-octane background and 3.3 wt% sulfur of DBT out of a iso-octane/toluene (85*v*:15*v*) mixture.[7] Also Cu_3BTC_2 has been proven to be an excellent adsorbent for organo-sulfur compounds in several studies.[14,15,9]

In this paper we focus on the isostructural CPO-27 series[16–18] (Cu, Zn, Mg, Co, Ni) as a promising family of adsorbents for the deep desulfurisation of fuels, alongside Cu_3BTC_2 and zeolite NaY as reference materials. CPO-27, also known as MOF-74, belongs to the class of MOFs with coordinatively unsaturated (*cus*) open-metal sites.[16] The honeycomb structure is composed of 2,5-dihydroxy-1,4-benzenedicarboxylate (DHBDC) organic linkers coordinated to X^{2+} divalent metal ions (where X^{2+} stands for Zn^{2+}, Mg^{2+}, Cu^{2+}, Co^{2+} and Ni^{2+}).[16,19,20] The one-dimensional hexagonal channels are about 12 Å in diameter. The impact of the metal cations on the adsorptive desulfurization is evaluated with a combination of adsorption isotherms, IR-spectroscopy, microcalorimetry and DFT calculations in order to obtain a full understanding of the interactions of S-heterocycles with the framework.

Materials, models and methods

Materials synthesis and characterization

CPO-27(Ni), CPO-27(Co), CPO-27(Mg), CPO-27(Zn) and CPO-27(Cu) were synthesized according to literature procedures.[21–24] The synthesis solvent was removed by washing the material seven times with methanol over a period of five days. Powder XRD patterns (Figure S1) were recorded on a STOE STADI P Combi instrument in Debye Scherrer geometry (Cu Kα1) using an IP position-sensitive detector (2θ=0–60°; $\Delta 2\theta$=0.03°).

Batch adsorption

Liquid phase batch adsorption experiments were carried out at 298 K in 1.8 ml glass vials filled with 0.025 g of adsorbent and a solution of heptane:toluene (80*v*:20*v*) contaminated with heteroaromatic sulphur compounds (0.005-0.5 M) following a literature procedure.[25] Uptakes were directly calculated from gas chromatography (GC) output data. In a standard procedure, the materials were pretreated at 523 K in an oven overnight under vacuum (< 10^{-5} bar). Adsorption isotherms were constructed by plotting the uptake, in weight%, vs. the residual concentration in solution. The initial slopes of the isotherms were determined by fitting a straight line through the first data points including the origin with regression coefficients R^2 exceeding 0.96. The separation factor α between a preferred compound A (thiophene) and a lesser adsorbed compound B (toluene) is defined as $\alpha = (y_A/y_B) / (x_A/x_B)$, with y the mole fractions in the adsorbed phase and x the mole fractions in the solution, both at equilibrium. For the determination of the temperature dependency of the separation factor, α is determined in the temperature range of 298-343K starting from equimolar mixtures of thiophene and toluene (0.5 M).

IR-spectroscopy

The infrared spectra were recorded using either a Perkin Elmer Spectrum GX IR spectrometer system or a Bruker Equinox 55 spectrometer (equipped with an MCT detector) with a spectral resolution of 2 cm^{-1}. A self-supporting wafer was prepared and evacuated at 250°C. All samples were normalized to the same sample mass: 10 mg (wafer density 3.2 mg/cm^2). For mass normalization the unperturbed lattice vibrations (bands at 1240, 1120 and 490 cm^{-1}) with maxima depending linearly on the sample mass were taken as the reference. IR adsorption measurements were repeated twice for each sample to ensure repeatability of the results and confirm homogeneity of the samples. Thiophene was adsorbed at room temperature from the vapor phase and the weakly physisorbed species were evacuated at room temperature, after which the spectrum was recorded.

Microcalorimetry

In each experiment, 0.025 g of sample was placed in a stainless steel ampule and activated under vacuum for 12 h at 523 K. After activation, 800 µL of a heptane:toluene (80:20) solution was added through a septum, and the ampule with the stirred suspension was loaded into the TAM III calorimeter (TA Instruments). An ampule with only the solvent was used as a reference. In the isothermal titration calorimetry (ITC), the liquid titrant (adsorbate) is added to the reaction ampule using a motor driven syringe pump via a fine cannula, and the heat flow is measured versus time until equilibrium is reached for each step. A total volume of 200 µL was added in steps of 10 µL. The integrated heats correspond to the adsorption and dilution phenomena ($Q_{measured} = Q_{adsorption} + Q_{dilution}$). In order to subtract the heat exchange due to dilution, an experiment without the sample is performed using the same conditions. For each injection, the corresponding equilibrium concentration was determined from adsorption isotherms determined on samples activated in identical conditions.

DFT calculations

Calculations on CPO-27(X) were performed with a trigonal primitive UC containing 162 framework atoms ($a = b = 25.9$ Å, $c = 6.8$ Å, $\alpha = \beta = 90°$, $\gamma = 120°$). Metal cations and DHBDC form helical chains along the *c* axis with the closest metal-metal distance $r(X_2\text{-}X_3) = \sim 2.9$ Å. Each X^{2+} centre is pentacoordinated to adjacent oxygen atoms from deprotonated hydroxyl or carboxylate groups of the organic linker to form a pseudo-square-pyramidal environment. The remaining sixth coordination site is accessible for an adsorbate molecule. Each of the three neighbouring metal cations (along the *c*-direction) points into one of the three adjacent channels. The distance between two adjacent *cus* sites accessible from the same channel is $r(X_1\text{-}X_4) = \sim 6.8$ Å and this distance represents the unit cell (UC) dimension along the *c*-direction.[26] The periodic structures with and without adsorbate molecules were optimized with respect to all atomic positions but with fixed lattice parameters; a high-spin electronic configuration on each X^{2+} ion was considered (see supporting information). All calculations with periodic DFT models were performed using the vdw-DF_2 exchange-correlation functional which accounts for dispersion interactions.[27] The projector augmented wave approximation (PAW)[28] and the plane wave basis set with a kinetic energy cutoff of 600 eV were used; a (1 × 1 × 2) Γ-centered grid of *k*-points was used for Brillouin-zone sampling. Periodic calculations were performed with the VASP 5.2.12 program. Calculations of lateral interactions were performed with a UC doubled along *c* and Γ point sampling.

Lateral thiophene-thiophene interactions within the CPO-27(X) framework were evaluated (i) along the *c*-axis (Figure S2a), and (ii) across the channel (Figure S2b). The lateral interactions of thiophenes organized in a stacked position along the c-axis were calculated as a difference in the interaction energy of one and two molecules adsorbed in a double UC. The average interaction energy per thiophene molecule at higher coverage is obtained as the arithmetic average for n adsorbate molecules within the UC.

To verify the accuracy of the DFT calculations, a small cluster model representing the closest environment of the *cus* site in CPO-27(X) was used. The cluster model is denoted as $F_2W(X)$, where F2 stands for two formyl (HCOO-) groups which are bound through oxygen atoms to the metal X^{2+} ions (X^{2+} = Zn^{2+}, Mg^{2+}, Cu^{2+}, Co^{2+} and Ni^{2+}) and W stands for a water molecule located in the fifth coordination site. The $F_2W(X)$ model is constrained to C_{2v} symmetry. The sixth coordination site remains accessible for an adsorbate. Thiophene interacting with the cluster model is denoted as $F_2W(X)$-S. Cluster model geometries of $F_2W(X)$ and $F_2W(X)$-S were optimized with a Perdew-Burke-Ernzerhof (PBE) exchange-correlation functional[29] and VTZ basis set in the high-spin configuration (see SI). The reported interaction energies (Table S2) are corrected for a basis set superposition error using the counterpoise correction method.[30] Accurate *ab initio* CCSD(T)/CBS calculations were performed at PBE/VTZ geometries. The complete basis set (CBS) extrapolation was evaluated based on the two-point Helgaker's extrapolation scheme ($E_X^{corr} = E_{CBS}^{corr} + AX^{-3}$) with AVDZ/AVTZ basis sets.[31] The extrapolation expresses the dependence of a correlation part of energy (*corr*) on a cardinal number X (D and T for double- and triple-ζ basis set, respectively). The HF/AVTZ energy was taken as the CBS limit for the uncorrelated part of the energy. The interaction energies at CCSD(T)/CBS level were obtained as: $E_{CCSD(T)/CBS} = E_{CCSD(T)/AVDZ}^{corr} + E_{MP2/CBS}^{corr} - E_{MP2/AVDZ}^{corr} + E_{HF/AVTZ}$

All geometry optimizations of cluster models at DFT level were performed with G09[32] and all other cluster model calculations with the Molpro2010.1 program suit.[33]

A faujasite-type zeolite NaY was represented by the reduced UC with a composition $Si_{35}Al_{13}Na_{13}O_{96}$ having Si/Al = 2.69/1 and unit cell parameters $\alpha = \beta = \gamma = 60°$ and $a = b = c = 17.37$ Å.[34] The NaY zeolite contains extra-framework Na^+ cations in sites I, I', and II; only sites II located above the six-ring oxygen atoms inside the supercage are accessible for adsorption. All DFT calculations on periodic models of NaY were performed using the vdw-DF_2 functional, the projector augmented wave approximation (PAW) and the plane wave basis set with a kinetic energy cutoff of 600 eV; Brillouin-zone sampling was restricted to the Γ-point.

RESULTS

Adsorption isotherms. In order to evaluate the sulfur uptake capacity of the CPO-27 adsorbents with different metals, adsorption isotherms of thiophene (TPH), benzothiophene (BT), dibenzothiophene (DBT) and 4,6-dimethyldibenzothiophene (DMDBT) are recorded out of a simulated fuel (heptane:toluene, 80:20). These S-heterocycles are representative molecules for the S-compounds typically found in fuels.[15,35] The different adsorption isotherms are presented in Figure 1.

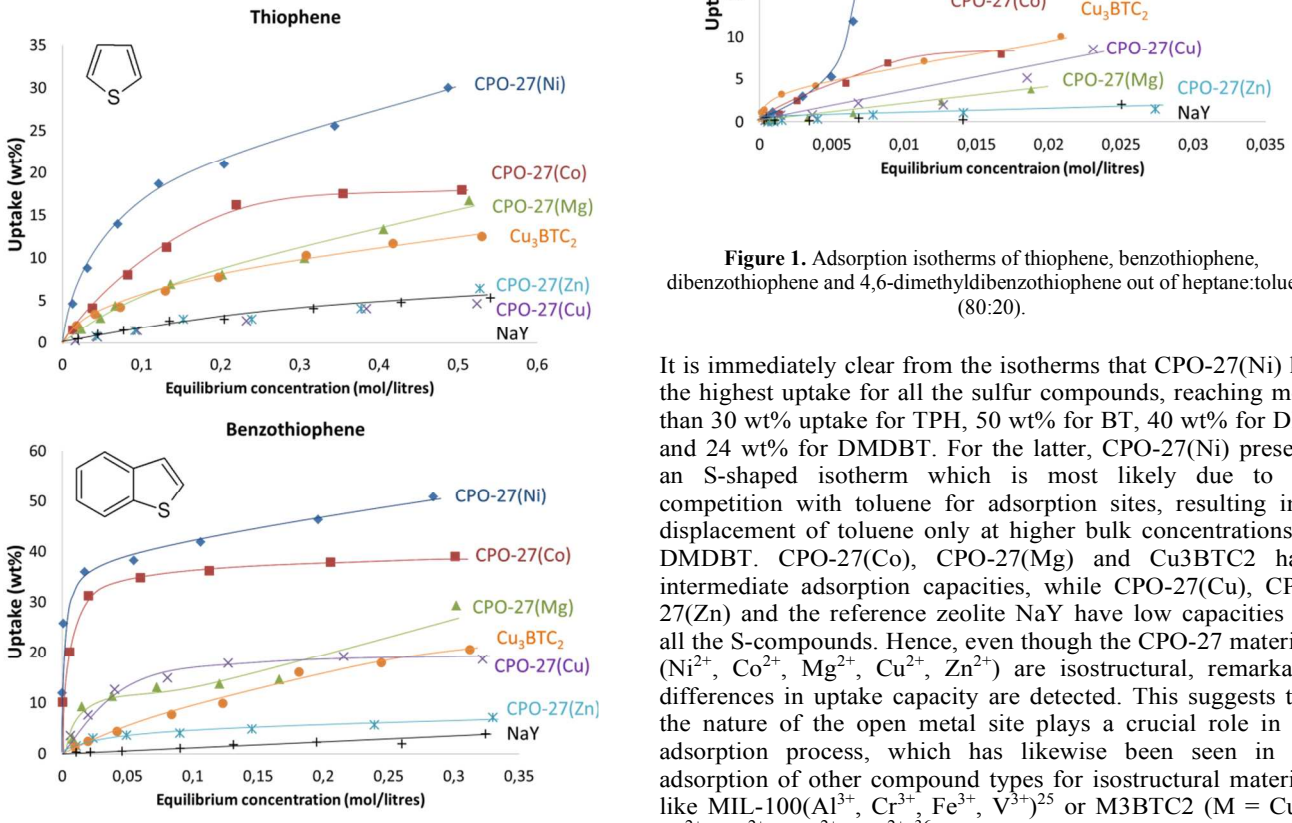

Figure 1. Adsorption isotherms of thiophene, benzothiophene, dibenzothiophene and 4,6-dimethyldibenzothiophene out of heptane:toluene (80:20).

It is immediately clear from the isotherms that CPO-27(Ni) has the highest uptake for all the sulfur compounds, reaching more than 30 wt% uptake for TPH, 50 wt% for BT, 40 wt% for DBT and 24 wt% for DMDBT. For the latter, CPO-27(Ni) presents an S-shaped isotherm which is most likely due to the competition with toluene for adsorption sites, resulting in a displacement of toluene only at higher bulk concentrations of DMDBT. CPO-27(Co), CPO-27(Mg) and Cu3BTC2 have intermediate adsorption capacities, while CPO-27(Cu), CPO-27(Zn) and the reference zeolite NaY have low capacities for all the S-compounds. Hence, even though the CPO-27 materials (Ni^{2+}, Co^{2+}, Mg^{2+}, Cu^{2+}, Zn^{2+}) are isostructural, remarkable differences in uptake capacity are detected. This suggests that the nature of the open metal site plays a crucial role in the adsorption process, which has likewise been seen in the adsorption of other compound types for isostructural materials like MIL-100(Al^{3+}, Cr^{3+}, Fe^{3+}, V^{3+})[25] or M3BTC2 (M = Cu^{2+}, Cr^{2+}, Ni^{2+}, Mo^{2+}, Ru^{2+})[36]. The occupation of the open metal sites (*cus*) of the CPO-27 series at saturation is therefore calculated and presented in Table 1.

Table 1. Percentage of the *cus* occupied at saturation.

	TPH	BT	DBT	DMDBT
CPO-27(Ni)	56 %	59 %	34 %	17 %
CPO-27(Co)	34 %	45 %	17 %	6 %
CPO-27(Mg)	24 %	27 %	11 %	2 %
CPO-27(Cu)	10 %	27 %	11 %	6 %
CPO-27(Zn)	12 %	9 %	10 %	1 %

As expected, CPO-27(Ni) has the highest occupation of the metal sites at saturation for all the different heterocycles. For a particular metal, the occupation of *cus* at saturation increases when going from TPH to BT. This is likely due to the phenyl ring of BT, which allows additional dispersion interactions with the framework.[37] The aromatic fraction in the fuel (simulated by admixture of toluene) will compete with the heterocycles for adsorption sites, as the phenyl ring can interact either with the metal cation or with the framework aromatic linkers.[38] The higher S uptake of CPO-27(Ni) compared to the other materials, indicates that the S-heteroaromatics compete more successfully for the open Ni sites than toluene. For materials saturated with DBT and DMDBT a decrease in *cus* occupation is detected, due to steric hindrance at higher occupation of the *cus* sites. Recall that the distance between two accessible *cus* is only 6.8 Å[37,26], while the kinetic diameter of DBT is estimated at ~9 Å.

Additional information can be obtained from the shape of the isotherm, as a steep uptake at low concentration means a high affinity for these compounds, which is of high importance with respect to removal of low concentrations of S-heteroaromatics.[3] A steep uptake is especially observed for CPO-27(Ni) as seen in Figure 2. By fitting a straight line through the low concentration domain of the isotherms, the affinity of the framework for the S-heterocycles can be calculated as the slope of the fit (L mol^{-1}).[9,25] For TPH, the affinity of the different CPO-27s is presented in Figure 2 and the values for all S-compounds are presented in Table S1.

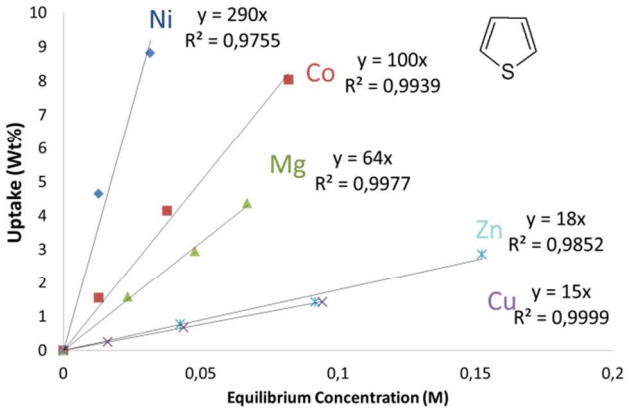

Figure 2. Affinities of CPO-27(Ni, Co, Mg, Zn, Cu) for thiophene out of heptane:toluene (80:20).

Similar as for the uptake capacities, CPO-27(Ni) has the highest affinity for all S-compounds tested (Table S1). CPO-27(Cu) and especially CPO-27(Zn) have very low affinities for most S-compounds. An interesting observation is the increased affinity of CPO-27(Ni) for the larger S-heterocycles: TPH < BT < DBT (Table S1). It is possible that for the larger heterocycles, the increased electron density on the sulfur atom[39] or the additional dispersion interactions enhance the initial affinity of the framework for the S-compounds. It should be noted that the lower affinity for DMDBT is most likely due to steric hindrance caused by the methyl groups in the 4,6-positions, making approach to and coordination on the *cus* more difficult. Overall, the very high affinity of CPO-27(Ni) allows strong reductions of the sulfur concentration, for instance from 130 ppm S to less than 1 ppm S, in the case of DBT, using 2.5 g of adsorbent per liter. Such performance allows to meet the stringent requirements for S concentrations in fuels even in the presence of other aromatics.

In order to understand the preference of CPO-27(Ni) for the S-heterocycles in the presence of aromatics like toluene, the temperature dependency of the separation factor for TPH or DBT over toluene is investigated. If a compound *A* is preferred over *B* only because the adsorption enthalpy of *A* is more negative than that of *B*, one would expect the separation factor to decrease with increasing temperature, according to Van 't Hoff's law.[40] The separation factor for the adsorption of thiophene/toluene from heptane on CPO-27(Ni) as a function of temperature is presented in Figure 3. The separation factor remains almost constant ($\alpha \approx 18$) in the temperature range of 298-343 K, indicating that besides the enthalpies, entropy effects play a significant role when dealing with the coadsorption of thiophene and toluene. For DBT the separation factor even increases with temperature suggesting a strong influence of entropy. Considering the molecular size of DBT, the adsorption of DBT will most likely displace two toluene molecules, thereby increasing the overall entropy of the system significantly upon adsorption of DBT.

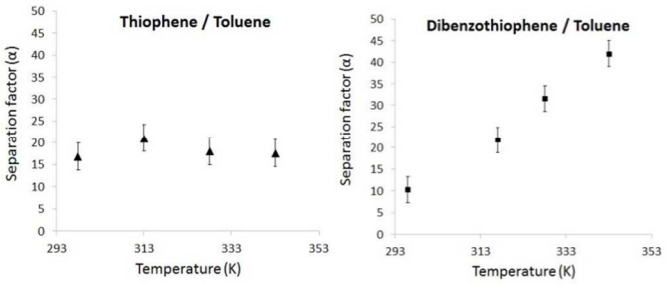

Figure 3. Temperature dependence of the separation factor for the empirical equimolar (at 0.4 M) thiophene/toluene separation on CPO-27(Ni).

The adsorption data clearly indicate that CPO-27(Ni) is a promising candidate for the deep removal of sulfur compounds from fuel feeds, by combining a high uptake capacity and strong affinity for all the tested compounds even in the presence of an aromatic background. Therefore, TPH is chosen as a model compound to further investigate the adsorption mechanism and the peculiar differences between the different metals in the CPO-27 series, by using a combination of microcalorimetry, IR-spectroscopy and DFT calculations.

Microcalorimetry. In order to quantify the affinity of the CPO-27 framework for thiophene, microcalorimetry was performed

for the materials with the highest uptake: CPO-27(Ni), CPO-27(Co) and CPO-27(Mg). The integral adsorption enthalpies as a function of the equilibrium concentration are plotted in Figure S3. CPO-27(Ni) has the highest integral adsorption enthalpy reaching 21 kJ mol^{-1}, followed by CPO-27(Co) with 7 kJ mol^{-1} and CPO-27(Mg) with 2.5 kJ mol^{-1}. These values may seem small, but recall that the value includes the differences in thiophene and toluene interaction energies and solvation energies in *n*-heptane. This observation confirms that the high affinity is directly related to the heat of adsorption, suggesting an enthalpic, coordinative interaction with the open metal site.[25]

FTIR spectroscopy. The pretreatment of the material is of critical importance, especially to remove strongly coordinating species left after the synthesis and to generate open metal sites. It is well known from literature that the pretreatment of the CPO-27 series is not without difficulties;[20] the materials were sufficiently washed with methanol and heated up to 250°C under vacuum (< 10^{-5} bar) to remove residual solvent molecules from the framework. The IR spectra confirm that the chosen conditions are sufficient to remove residual species from the pores, as no superfluous MeOH or DMF signals can be detected (Figure S4). The interaction strength of thiophene with the different CPO-27 frameworks was further analyzed with IR by monitoring the adsorption of thiophene at room temperature out of vapour phase (80 mbar) on a self-supporting wafer. By comparing the intensities of the out-of-plane C-H bending[41] between 730-680 cm^{-1} after evacuation (Figure S5), the interaction strength of the thiophene adsorption can at least qualitatively be assessed. Although the precise order of IR intensity for the different metals is not exactly the same as in the adsorption isotherms, the strong interaction of thiophene with CPO-27(Ni) is confirmed spectroscopically.

DFT calculations. The reliability of DFT methods for the description of thiophene interaction with CPO-27(X) MOFs was tested using a small $F_2W(X)$ cluster model (Figure S2c). Interaction energies calculated at various levels of theory using the PBE-optimized geometry are summarized in Table S2. Following observations can be made with respect to the reference CCSD(T)/CBS level of theory: (i) the vdW-DF_2 functional gives interaction energies in excellent agreement with CCSD(T) except for the Ni^{2+} cluster (see below), (ii) the PBE functional understimates the interaction and B3LYP completely fails to describe the interaction, (iii) MP2/CBS interaction energies agree well with those obtained using CCSD(T)/CBS; a very strong dependence of the results on the basis set size is noted. The rather short bond length of 2.45 Å between Ni^{2+} and S indicates a covalent character of the interaction (compare the sum of Van der Waals and covalent radii for Ni and S, 3.43 and 2.29 Å, respectively). The covalent interaction between Ni^{2+} and thiophene is overestimated with the vdW-DF_2 functional while the PBE functional (failing for all other complexes) describes this interaction well.

The interaction of thiophene with CPO-27(X) represented by periodic models is increasing in the order Zn^{2+} < Cu^{2+} < Mg^{2+} < Co^{2+} < Ni^{2+}, ranging from -49 (Zn^{2+}) to -61 (Ni^{2+}) kJ mol^{-1} (Table 2). While the interaction with thiophene was considered for all adsorbents investigated herein, the interaction with DBT and toluene was considered only for a selected subset of adsorbents, which results in a sufficient qualitative understanding. The interaction energies calculated with periodic models are about 40 kJ mol^{-1} larger than those obtained with cluster models, indicating a dominant role of dispersion interactions. The contribution of dispersion interactions to the total interaction energy was estimated as the difference between the interaction energy calculated with vdW-DF_2 and PBE functionals and periodic models, corrected for the deficiency of the PBE functional obtained with cluster models (Table S2). These estimations result in 35 and 38 kJ mol^{-1} for CPO-27(Zn) and CPO-27(Mg), respectively. This allows to ascribe ~ 70% of the interactions between thiophene and CPO-27 to dispersion interactions.

The large role of dispersion interactions also influences the structure of the thiophene adsorption complexes. For the cluster models, the metal-S distances are in the range of 2.49-3.54 Å, while the geometries obtained with the periodic model (Table S2) for various metal cations are relatively similar, ranging from 2.75 Å (Ni^{2+}–S) to 3.16 Å (Zn^{2+}–S). The geometry of the thiophene adsorption complexes in CPO-27(Ni) is shown in Figures 4 and 5; in addition to the interaction with the *cus* site, thiophene also interacts with the aromatic rings of the organic linkers, forming a stacked complex. The dispersion interaction with the organic linker compensates well for a partial loss of electrostatic interaction between *cus* and thiophene because of the thiophene leaning towards the organic linker (angle α, Table 3); distances between thiophene and linker atoms are as small as 3.6 – 3.8 Å.

Table 2. Interaction energies of TPH, DBT and toluene with CPO-27(X) adsorbents[a] calculated with periodic DFT for low coverage.

	ΔE_{int}			Geometry (TPH)	
System	TPH[b]	DBT	Toluene	r(XS)[c]	α[d]
CPO-27(Zn)	-48.8			3.161	138.4
CPO-27(Cu)	-51.1			3.105	124.2
CPO-27(Mg)	-55.4	-129.9	-71.0 (-57)[e]	3.041	127.0
CPO-27(Co)	-55.9			2.925	128.5
CPO-27(Ni)	-60.5	-135.8	-70.3 (-56)[e]	2.749	127.9

[a] In kJ mol^{-1}; vdw-DF2 functional, energy cut-off 600 eV. [b] Reported interaction energies after subtraction of lateral interactions. [c] X^{2+}-S distance in Å; Figure 5a.[d] α is the angle between the X^{2+}-S bond and the plane of the thiophene aromatic ring; Figure 5b. [e] Interaction energy of toluene corrected for the differences in solvation energy in *n*-heptane (with respect to thiophene).

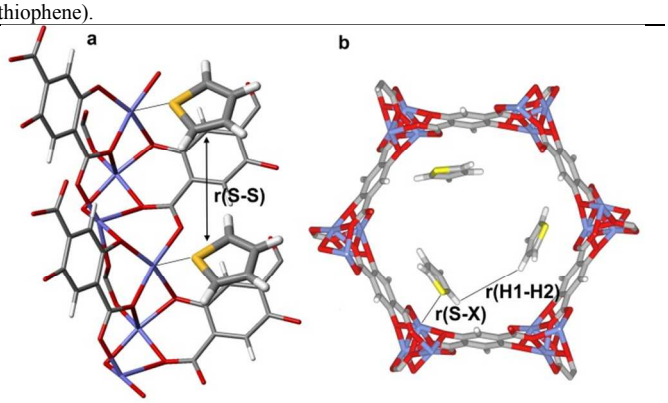

Figure 4. Lateral interactions between thiophene molecules adsorbed in CPO-27. (a) Two molecules of thiophene bound on *cus* sites along the channel direction. (b) Three molecules of thiophene bound in one hexagonal channel in one unit cell.

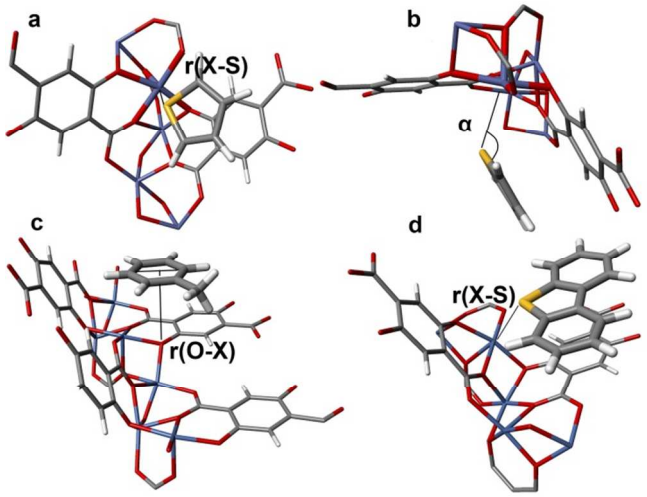

Figure 5. The structure of thiophene adsorbed on the *cus* site of CPO-27(Ni) viewed along [010] and [001] directions (parts a and b, respectively). The structure of the toluene (c) and DBT (d) adsorption complexes in CPO-27(Ni).

Considering the high density of *cus* sites in CPO-27, the lateral interactions between adsorbed thiophenes were evaluated at the vdW-DF_2 level. The closest *r*(S-S) distance between two thiophene molecules adsorbed on adjacent *cus* sites in the same channel along the *c* direction in CPO-27(Ni) is 6.837 Å (Figure 4a). This leads to additional stabilization of adsorbed thiophene due to lateral interactions (5.8 kJ mol^{-1}). Maximally three molecules can fit inside one channel of the UC at higher coverages (Figure 4b), making the maximum adsorption capacity for the primary adsorption sites around 50 % occupation of the *cus*. This agrees excellently with the empirically found value (56%, see Table 1) for the adsorbent with the highest uptake capacity at saturation, viz. CPO-27(Ni). The lateral interaction of -2.7 kJ mol^{-1} calculated for a pair of thiophene molecules in such arrangement corresponds to increased interaction energies at higher coverages.

The adsorption of DBT and toluene on CPO-27(Mg) and CPO-27(Ni) was also investigated in order to confirm the preferred adsorption of S-heterocyclic compounds from the toluene/heptane liquid phase (20:80) background. Toluene interaction energies for CPO-27(Mg) and CPO-27(Ni) are very similar, -70 kJ mol^{-1} and -71 kJ mol^{-1}, respectively (Table 2). Therefore, the interaction of toluene with CPO-27 does not seem to depend strongly on the metal ion X^{2+}. On the contrary, the interaction energies for DBT with CPO-27(Mg) and CPO-27(Ni) are -130 kJ mol^{-1} and -136 kJ mol^{-1}, respectively (Table 2). Compared to the thiophene interactions (see above) DBT is bound significantly stronger to CPO-27 (by about 75 kJ mol-1) due to additional stabilization by dispersion interactions between the two aromatic rings of DBT and CPO-27 framework atoms (Figure 5d). Interaction energies of DBT with CPO-27(Mg) and CPO-27(Ni) follow the same trend as reported above for thiophene.

The experimental adsorption isotherms and microcalorimetry reflect the equilibrium that can be simply described as: $(Toluene)_{ads} + (Thiophene)_{solv} \leftrightarrow (Thiophene)_{ads} + (Toluene)_{solv}$; where subscripts *ads* and *solv* refer to the molecule adsorbed on the cationic site in the MOF and to the molecule solvated in a 20:80 toluene/heptane mixture. Since no relevant solvation energies could be found in literature they were calculated using continuum solvation SMD model.[42] The solvation of toluene in n-heptane was found 14 kJ mol^{-1} more favourable than solvation of thiophene.

Discussion

The trends obtained from theoretical and experimental observations are clear: CPO-27(Ni) is in all cases the best performing material, both regarding capacity and affinity at low concentrations. When comparing the sulfur uptake capacities (in wt% S) with those of reference materials (Table 3), a significantly higher adsorption capacity is obtained for the CPO-27(Ni). The adsorption capacity of MOF-505 for DBT (3.3 wt% S) and DMDBT (0.9 wt% S) previously reported by Matzger *et al.*, is surpassed by CPO-27(Ni) reaching 6.9 and 3.6 wt% S for DBT and DMDBT, respectively. The superior performance in comparison with the reference materials Cu_3BTC_2, NaY zeolite and other state-of-the-art adsorbents, like the Cu-exchanged Y zeolite, active carbon or the Ni-loaded SiO_2-Al_2O_3, confirms the remarkable performance of the CPO-27(Ni) material (Table 3). These results are in line with the previously obtained data on the adsorption of thiophene from n-octane on CPO-27(Ni) by Peralta *et al.* Furthermore, our data confirm their previous findings on the stability of CPO-27(Ni), as an easy solvent regeneration with toluene results in a similar uptake capacity for thiophene in several consecutive adsorption cycles (Figure S6).

Table 3. Overview of adsorption capacity for S-heterocycles for various microporous materials achieved under similar experimental conditions.

	Maximum uptake sulfur compounds (wt% S)				
	TPH	BT	DBT	DMDBT	REF
Ni/SiO_2-Al_2O_3	/	/	0.22	0.13	43
Activated Carbon	/	/	0.80	1.1	43
CPO-27(Ni)	11.4	12	6.9	3.6	This work
MOF-505	/	/	3.3	0.9	7
MIL-100(Fe)	1.5	1.4	1.2	/	9
CuY	1.4	/	/	/	13
Cu_3BTC_2	4.8	4.9	4.6	1.8	This work
NaY	2.0	0.5	0.6	0.2	This work

For the variously metallated CPO-27(X) materials, the interaction energies with the S-heterocycles, as obtained by calculation, quite precisely reflect the empirically observed order; this indicates that the differences between the metals can be rationalized based on the interaction energy between the S-heterocycle and the metal *cus*. For the best material, CPO-27(Ni), it is shown that the Ni-S interaction has a partially covalent nature; but besides the metal-S interaction, dispersive interactions are important as well. This lines up nicely with the large interaction energies calculated for dibenzothiophene (DBT), which is also empirically found to be more strongly adsorbed than thiophene.

While qualitative agreement between experimental and theoretical results is obvious, quantitative agreement cannot be reached simply by comparing calculated interaction energies with experimental data. Indeed, the calculated interaction energies of toluene (-70 kJ mol^{-1}) is larger than that of thiophene (-60 kJ mol^{-1} for Ni^{2+}); however, accounting for the differences in solvation energies in *n*-heptane reverses this order (values in parentheses in Table 2). Improving the solvation model (considering the 80:20 heptane/toluene mixture) and accounting for the entropy contribution is expected to further shift relative energies in favour of heterocyclic compounds. Calculation also brings forward that even in comparison with an aromatic solvent molecule such as toluene, DBT is clearly preferred. Considering that the distance between two accessible *cus* is only 6.8 Å[37,26], while the kinetic diameter of DBT is estimated at ~9 Å, the adsorption of DBT will displace two toluene molecules to the bulk solution and thereby increase the entropy of the system significantly.

The temperature independency of the separation factor of equimolar mixtures suggests that additional effects play a role, besides an enthalpy driven sulfur-metal interaction. First, the lower solubility of thiophene compared to that of toluene in heptane can result in a larger driving force for thiophene to leave the apolar solvent. Secondly, adsorption of thiophene and toluene in the pores of CPO-27 may result in entropically different situations. When a polar compound like thiophene transfers from an apolar solvent to CPO-27 the entropy loss of the overall system (including the adsorbent) will be smaller compared to the entropy loss when an apolar molecule like toluene leaves the apolar solvent.[44,45]

Conclusion

By combining experimental adsorption isotherms, microcalorimetric data, IR spectroscopy and quantum chemical calculations a detailed insight into the adsorption preference and mechanism for sorption of S-heteroaromatics on CPO-27 type materials is obtained. CPO-27(Ni) is one of the best S-adsorbents found in literature; it outperforms the other CPO-27 materials due to a better sulfur-metal interaction, even though more than 70 % of the interaction energy of the sulfur compounds with the framework originates from dispersive interactions. Furthermore, for S-heterocycles adsorption in CPO-27(Ni) entropy effects are important, especially when toluene, as a component of the solvent mixture, competes for adsorption sites.

Acknowledgements

The work has been funded by MACADEMIA (www.macademia-project.eu). MACADEMIA is a 4-year Large-scale Integrating Collaborative Project, funded under the EU Seventh Framework Programme for Research and Development, under the Nanosciences, Nanotechnologies, Materials and New Production Technologies Theme ([FP7/2007-2013] under grant agreement n° 228862). P.N. and M.H. acknowledge the Czech Science Foundation for the support (14-07101S) and for the calculations MetaCentrum and CERIT-SC computational facilities (MSM/LM2010005 and OP VaVpI CZ. 1.05/3.2.00/08.0144). D.D.V. is grateful for support to FWO (research projects), to KULeuven (Metusalem CASAS funding), to IWT (MOFShape SBO grant 110050). The IR studies (B.G. and B.M.) were carried out with the equipment purchased thanks to the financial support of the European Regional Development Fund in the framework of the Polish Innovation Economy Operational Program (contract no. POIG.02.01.00-12-023/08). B.M. also thanks the Polish National Science Center for funding (grant no. 2013/11/N/ST5/01302) and funding from Marian Smoluchowski Kraków Research Consortium – a Leading National Research Centre KNOW supported by the Ministry of Science and Higher Education.

Notes and references

[a] Centre for Surface Chemistry and Catalysis (COK), KU Leuven, Arenbergpark 23, B-3001 Leuven (Belgium)
[b] Department of Physical and Macromolecular Chemistry, Faculty of Science, Charles University in Prague, Hlavova 2030/8, 128 43 Prague (Czech Republic)
[c] Faculty of Chemistry, Jagiellonian University, ul. Ingardena 3, 30-060 Kraków (Poland)
[d] CNRS, Lab. Chimie Provence, Madirel, Université Aix-Marseille, 1-3, UMR 6264, MATDIV Grp, Ctr St Jerôme, F-13397 Marseille 20 (France)
* corresponding author: dirk.devos@biw.kuleuven.be

† Electronic Supplementary Information (ESI) available: [Details about the computational modelling and additional figures]. See DOI: 10.1039/b000000x/

REFERENCES
1. J.-R. Li, J. Sculley, and H.-C. Zhou, *Chem. Rev.*, 2012, **112**, 869–932.
2. J.-R. Li, R. J. Kuppler, and H.-C. Zhou, *Chem. Soc. Rev.*, 2009, **38**, 1477–504.
3. R. T. Yang, *Adsorbents: FUNDAMENTALS AND APPLICATIONS*, 2007.
4. H. Wu, Q. Gong, D. H. Olson, and J. Li, *Chem. Rev.*, 2012, **112**, 836–68.
5. Z. R. Herm, E. D. Bloch, and R. Long, *Chem. Mater.*, 2014, **26**, 323–338.
6. B. Van de Voorde, B. Bueken, J. Denayer, and D. De Vos, *Chem. Soc. Rev.*, 2014, **43**, 5766–5788.
7. K. A. Cychosz, A. G. Wong-Foy, and A. J. Matzger, *J. Am. Chem. Soc.*, 2008, **130**, 6938–9.
8. B. Van de Voorde, A. Munn, N. Guillou, F. Millange, D. E. De Vos, and R. I. Walton, *Phys. Chem. Chem. Phys.*, 2013, **15**, 8606–8615.
9. M. Maes, M. Trekels, M. Boulhout, S. Schouteden, F. Vermoortele, L. Alaerts, D. Heurtaux, Y.-K. Seo, Y. K. Hwang, J.-S. Chang, I. Beurroies, R. Denoyel, K. Temst, A. Vantomme, P. Horcajada, C. Serre, and D. E. De Vos, *Angew. Chem. Int. Ed. Engl.*, 2011, **50**, 4210–4.
10. S. Achmann, G. Hagen, M. Hämmerle, I. M. Malkowsky, C. Kiener, and R. Moos, *Chem. Eng. Technol.*, 2010, **33**, 275–280.
11. V. Chandra Srivastava, *RSC Adv.*, 2012, **2**, 759.
12. S. K. Bej, S. K. Maity, and U. T. Turaga, *Energy & Fuels*, 2005, **18**, 1227–1230.
13. A. J. Hernández-Maldonado and R. T. Yang, *Catal. Rev.*, 2004, **46**, 111–150.
14. G. Blanco-Brieva, J. M. Campos-Martin, S. M. Al-Zahrani, and J. L. G. Fierro, *Fuel*, 2011, **90**, 190–197.
15. D. Peralta, G. Chaplais, A. Simon-Masseron, K. Barthelet, and G. D. Pirngruber, *Energy & Fuels*, 2012, **26**, 4953–4960.
16. N. L. Rosi, J. Kim, M. Eddaoudi, B. Chen, M. O'Keeffe, and O. M. Yaghi, *J. Am. Chem. Soc.*, 2005, **127**, 1504–18.
17. P. D. C. Dietzel, Y. Morita, R. Blom, and H. Fjellvåg, *Angew. Chem. Int. Ed. Engl.*, 2005, **44**, 6354–8.
18. P. D. C. Dietzel, V. Besikiotis, and R. Blom, *J. Mater. Chem.*, 2009, **19**, 7362.
19. P. D. C. Dietzel, B. Panella, M. Hirscher, R. Blom, and H. Fjellvåg, *Chem. Commun. (Camb).*, 2006, **1**, 959–61.

20. P. D. C. Dietzel, R. Blom, and H. Fjellvåg, *Eur. J. Inorg. Chem.*, 2008, **2008**, 3624–3632.
21. P. D. C. Dietzel, V. Besikiotis, and R. Blom, *J. Mater. Chem.*, 2009, **19**, 7362–7370.
22. S. R. Caskey, A. G. Wong-Foy, and A. J. Matzger, *J. Am. Chem. Soc.*, 2008, **130**, 10870–1.
23. J. L. C. Rowsell and O. M. Yaghi, *Microporous Mesoporous Mater.*, 2004, **73**, 3–14.
24. R. Sanz, F. Martínez, G. Orcajo, L. Wojtas, and D. Briones, *Dalton Trans.*, 2013, **42**, 2392–8.
25. B. Van de Voorde, M. Boulhout, F. Vermoortele, P. Horcajada, D. Cunha, J. S. Lee, J.-S. Chang, E. Gibson, M. Daturi, J.-C. Lavalley, A. Vimont, I. Beurroies, and D. E. De Vos, *J. Am. Chem. Soc.*, 2013, **135**, 9849–56.
26. H. Wu, J. M. Simmons, G. Srinivas, W. Zhou, and T. Yildirim, *J. Phys. Chem. Lett.*, 2010, **1**, 1946–1951.
27. K. Lee, É. D. Murray, L. Kong, B. I. Lundqvist, and D. C. Langreth, *Phys. Rev. B*, 2010, **82**, 081101.
28. G. Kresse and J. Hafner, *Phys. Rev. B*, 1993, **48**, 13115–13118.
29. J. P. Perdew, K. Burke, and M. Ernzerhof, *Phys. Rev. Lett.*, 1996, **77**, 3865–3868.
30. S. F. Boys and F. Bernardi, *Mol. Phys.*, 1970, **19**, 553–566.
31. T. Helgaker, W. Klopper, H. Koch, and J. Noga, *J. Chem. Phys.*, 1997, **106**, 9639.
32. R. A. . Gaussian 09, M. J. Frisch, G. W. Trucks, H. B. Schlegel, G. E. Scuseria, M. A. Robb, J. Cheeseman, R. G. Scalmani, V. Barone, B. Mennucci, G. A. Petersson, H. Nakatsuji, M. Caricato, X. Li, H. P. Hratchian, A. F. Izmaylov, J. Bloino, G. Zhen, J. L. Sonnenberg, M. Hada, M. Ehara, K. Toyota, R. Fukuda, J. Hasegawa, M. Ishida, T. Nakajima, Y. Honda, O. Kitao, H. Nakai, T. Vreven, J. A. Montgomery, J. E. Peralta, F. Ogliaro, M. Bearpark, J. J. Heyd, E. Brothers, K. N. Kudin, V. N. Staroverov, R. Kobayashi, J. Normand, K. Raghavachari, A. Rendell, J. C. Burant, S. S. Iyengar, J. Tomasi, M. Cossi, N. Rega, J. M. Millam, M. Klene, J. E. Knox, J. B. Cross, V. Bakken, C. Adamo, J. Jaramillo, R. Gomperts, R. E. Stratmann, O. Yazyev, A. J. Austin, R. Cammi, C. Pomelli, J. W. Ochterski, R. L. Martin, K. Morokuma, V. G. Zakrzewski, G. A. Voth, P. Salvador, J. J. Dannenberg, S. Dapprich, A. D. Daniels, O. Farkas, J. B. Foresman, J. V. Ortiz, J. Cioslowski, and D. J. Fox, 2009.
33. M. is a package of ab initio programs written By, H.-J. Werner, P. J. Knowles, and et al., 2012.
34. L. Grajciar, J. Čejka, A. Zukal, C. Otero Areán, G. Turnes Palomino, and P. Nachtigall, *ChemSusChem*, 2012, **5**, 2011–22.
35. K. A. Cychosz, R. Ahmad, and A. J. Matzger, *Chem. Sci.*, 2010, **1**, 293.
36. C. Wade and M. Dincă, *Dalt. Trans.*, 2012, **41**, 7931–7938.
37. L. Valenzano, B. Civalleri, K. Sillar, and J. Sauer, *J. Phys. Chem. C*, 2011, **115**, 21777–21784.
38. L. Valenzano, B. Civalleri, S. Chavan, G. T. Palomino, C. O. Area, and S. Bordiga, *J. Phys. Chem. C*, 2010, **114**, 11185–11191.
39. S. Otsuki, T. Nonaka, N. Takashima, W. Qian, A. Ishihara, T. Imai, and T. Kabe, *Energy & Fuels*, 2000, **39**, 1232–1239.
40. M. Maes, F. Vermoortele, L. Alaerts, S. Couck, C. E. A. Kirschhock, J. F. M. Denayer, and D. E. De Vos, *J. Am. Chem. Soc.*, 2010, **132**, 15277–85.
41. F. Hegelund, R. Wugt Larsen, and M. H. Palmer, *J. Mol. Spectrosc.*, 2008, **247**, 100–114.
42. A. V. Marenich, C. J. Cramer, and D. G. Truhlar, *J. Phys. Chem. B*, 2009, **113**, 6378–6396.
43. J. H. Kim, X. Ma, A. Zhou, and C. Song, *Catal. Today*, 2006, **111**, 74–83.
44. N. F. A. van der Vegt and W. F. van Gunsteren, *J. Phys. Chem. B*, 2004, **108**, 1056–1064.
45. P. Jandera, K. Krupczyńska, K. Vynuchalová, and B. Buszewski, *J. Chromatogr. A*, 2010, **1217**, 6052–60.

